Formulation and Manufacture of Pharmaceuticals by Fluidized-Bed Impregnation of Active Pharmaceutical Ingredients onto Porous Carriers

Plamen I. Grigorov, Benjamin J. Glasser, and Fernando J. Muzzio
Dept. of Chemical and Biochemical Engineering, Rutgers, The State University of New Jersey, Piscataway, NJ 08854

DOI 10.1002/aic.14209
Published online September 12, 2013 in Wiley Online Library (wileyonlinelibrary.com)

A manufacturing method is presented for solid dosage forms using fluidized-bed impregnation, which could eliminate many of the challenges during solid dosage manufacturing. The main difference between impregnation and dry blending is the placement of the active pharmaceutical ingredient (API) inside a porous carrier. This makes the final material flow properties independent of the physical properties of the API. The method consists of spraying an API solution in appropriate solvent onto a carefully chosen porous excipient in a fluidized state. The solution penetrates the porous carrier due to capillary forces and the solvent is evaporated soon after that. Impregnation and drying occur simultaneously, which makes this impregnation method suitable for continuous implementation. Carefully choosing the operating conditions allows impregnation to occur without introducing spray drying or spray coating of the API. The method is shown to generate an impregnated excipient with very high degree of homogeneity independent of the API loading. It is also shown that mild milling further improves blend uniformity to RSD levels below 1%, which are challenging to achieve using conventional techniques. On impregnation, the final physical properties of the material are seen to be mainly unchanged from the initial excipient properties. A study of this one-step manufacturing method is described, using acetaminophen as the model drug and anhydrous calcium phosphate dibasic as the porous excipient. The experimental work presented establishes a proof of concept and investigates in detail blend uniformity, physical state of impregnated API, final physical properties of impregnated material, compressibility during tableting, capsule filling, and release profile of the final capsule formulation. It also discusses potential ways for drug release control and improvements using impregnation. *AIChE J*, 59: 4538–4552, 2013
Keywords: pharmaceutical, drug substance, impregnation, porous carrier, fluidized bed

Introduction

Approximately 65% of all prescription drugs are manufactured as solid dosage forms,[1] which includes tablets and capsules. In both cases the final formulation consists of an excipient (or mixtures of excipients) and an active pharmaceutical ingredient (API) which is homogeneously distributed throughout the excipient matrix. For very potent drugs, the amount of API in the solid dosage form can be as low as 0.1 wt %, or in some cases, even lower.[2] This very low API loading poses one of the biggest challenges in pharmaceutical product development: the control of dose uniformity. Low API content variability in the blend (or equivalently, a high level of blend homogeneity) are highly desired and strictly enforced by the U.S. Food and Drug Administration (FDA). Current guidelines developed by the FDA require API content variability in finished products to have relative standard deviation (RSD) of no higher than 6%, with lower being better.[3] Typically, the leading source of product content variability is poor blend uniformity. In the commonly available approaches for blend uniformity control (for example, direct blending followed by wet or dry granulation) as the API concentration decreases, the variability of the blend increases, which makes it very difficult to meet FDA's requirements for low-drug loadings. Therefore, a process or method that is able to tightly control API variability in blends, regardless of drug loadings, is very desirable.

Another important aspect of pharmaceutical process development is the final product cost. As pharmaceutical companies strive to develop more affordable drugs, any possible elimination of lengthy and expensive unit operations becomes commercially advantageous. One group of such unit operations is associated with the control of API attributes (size, size distribution, shape, bulk density, etc.). These unit operations can include crystallization control and various milling and delumping steps. The need for control of API attributes is solely dictated by the drug product development and usually is associated with desired improvements in blend uniformity or release profile. Having a formulation process that can make these and other steps unnecessary will

Correspondence concerning this article should be addressed to F. J. Muzzio at fjmuzzio@yahoo.com.

provide a large advantage to pharmaceutical companies and the whole industry.

One method for manufacturing that we believe could address all of the aforementioned challenges in drug substance and product development is impregnation of porous carriers. By definition, impregnation is the process of filling the internal void structure of a porous carrier with a chemical substance. Impregnation is a well-known process, which currently is generally used in supported catalyst preparation. Benefits of impregnation to catalyst manufacture include high uniformity of the dispersed active component (Ni, Pt, Pd, Co, etc) within the support (typically alumina or silica), chemical and mechanical stabilization of the active, increase in total active surface area and reduction in the amount of the catalyst metal (usually very expensive). There are two types of impregnation, namely dry (or capillary) impregnation and wet (or diffusional) impregnation.[4–7] As the name suggests, during dry impregnation the support is initially dry and the driving force for impregnation is capillarity. Liquid solution is drawn inside the carrier due to capillary forces. Similarly, during wet impregnation, the support is initially wetted with pure solvent and the driving force for impregnation is the concentration gradient. An important outcome of the impregnation process is the catalyst profile in the supported particles. There are four distinct types of catalyst profiles: uniform, egg-shell, egg-white and egg-yolk. These generally depend on the nature of the interactions (physical or chemical) between the support and catalyst. Several authors have shown that the catalyst profile determined during impregnation can be significantly altered during the drying phase.[4,6,8] Mathematical models describing catalyst profile control during drying have also been developed.[9–11]

Impregnation of APIs onto porous excipients has been gaining attention only in the past several years. Research activities in this area have been focused primarily on altering (increasing or decreasing) of the dissolution profile of the API. Many of today's drugs are poorly soluble in water and ways to increase their solubilities are becoming more attractive. Impregnation is a process that by design offers an unique approach for dissolution profile increase.[12,13] The increase in release kinetics comes from the fact that drug molecules are deposited in small pores, which increases the effective surface area for dissolution. In some cases, drug molecules are deposited in the form of an amorphous solid[14,15] or as a molecular dispersions.[12,13,16] Impregnation also offers a possibility for controlled-release formulations.[16,17]

There are three main types of impregnation techniques commonly used for loading of porous carriers with APIs. The most common of the three is the dry impregnation method already mentioned, also known as incipient wetness impregnation.[12,13,17,18] This method usually involves mixing of a dry porous carrier with an API solution in appropriate organic solvent and the subsequent evaporation of the solvent by drying (usually *in vacuo*). It is simple and easily achieved in the laboratory environment. One drawback of this method is that the final drug loading depends on its solubility in the organic solvent. If the solubility of the API is low then several impregnation-drying cycles could be needed to obtain the targeted drug loading in the carrier.

Another technique for impregnation gaining academic attention involves super critical CO_2 as the impregnation media.[16,19,20] Due to its low viscosity and ability to swell many polymers, supercritical CO_2 is particularly useful when impregnating APIs into biocompatible polymeric carriers. Its use is advantageous since it is nontoxic and easy to remove from the final product. However, the method often has as a drawback due to limited drug solubility in the supercritical CO_2. Another drawback of this method is the relatively high-capital cost if it is to be implemented on commercial scale.

A third, not very popular technique for impregnation is the melt method.[12,14,21] As the name suggest, the drug and porous carrier are mixed together and then heated above the melting point of the API. Being in a liquid form, the API penetrates inside the porous support drawn by capillary forces. There are two main drawbacks of this method. First, due to the usually high viscosity of many molten APIs, penetration within the porous matrix is slowed down. Second, not too many APIs are chemically stable in a molten state to undergo impregnation.

A fourth method for impregnation, which has not being widely used, involves dry impregnation of porous carriers in a fluidized bed (FB). It has been successfully demonstrated for the preparation of supported metal catalysts.[22–25] The method involves three steps, which occur simultaneously in a continuous fashion (1) API solution in appropriate solvent is sprayed onto a porous excipient in a fluidized state, (2) the API solution penetrates the porous carrier driven by capillary forces, and (3) the carrier particles loaded with API solution dry as they move around the bed. Desportes et al.[22] describes two characteristic times governing the impregnation process. These are the impregnation time (t_I), the time which is needed for the liquid to go from the external surface toward the particle center, and the drying time (t_D), the time which is needed for a particle saturated by pure solvent to be transformed into a dry particle. Impregnation is achieved when $t_D/t_I > 10$ and coating is achieved when $t_D/t_I < 10$. Controlling the spray rate, fluidization gas inlet temperature and flow rate ultimately control the impregnation process.

In this article, we present a study on a new method for formulation and manufacture of pharmaceuticals using fluidized-bed impregnation. To the best of our knowledge this method has never been used before for impregnation of APIs onto excipients. It has several advantages over current methods for impregnation. Fluidization of powders is a well-established unit operation used for drying, coating and granulation. It provides excellent mixing of excipient particles during impregnation. Fluidized bed (FB) impregnation often will not involve new capital, as any FB dryer/granulator can be used for impregnation with minimum retrofitting (provided the manufacturer already has such equipment).

In impregnation in a FB, impregnation and drying steps occur simultaneously. This makes the final targeted API loading independent of its solubility in the solvent used. In principle, low-concentration solutions just need to be sprayed for a longer time during FB impregnation and any targeted drug loading (up to the maximum determined by the pore volume of the carrier) could be achieved.

Fluidized-bed impregnation offers numerous advantages in drug manufacturing for solid dosage forms over the most common current methods (e.g., blending,[26] granulating, etc.). All of these advantages come from the fact that impregnation allows the API to be deposited inside the excipient particles vs. being distributed between them as it is the case with physical blending (patent pending[27]). Placing the API within the excipient allows for several benefits by design (1) surface properties of impregnated excipient remain almost

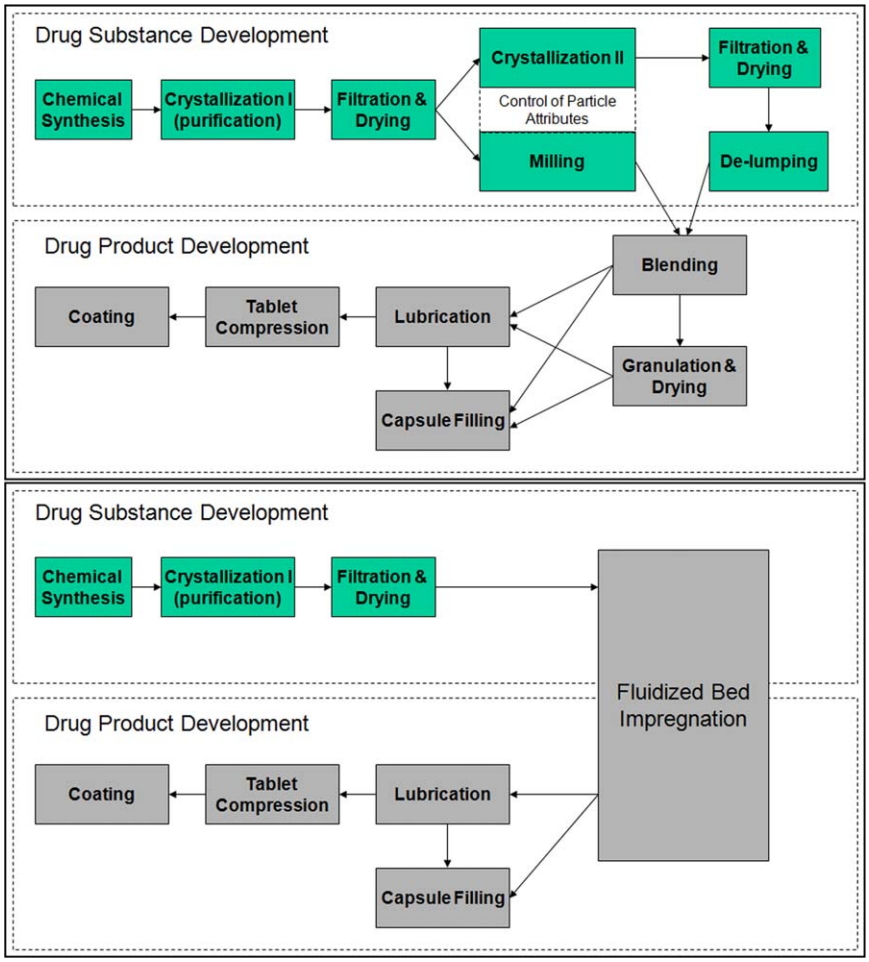

Figure 1. Summary of typical unit operations involved in the manufacture of solid dosage pharmaceuticals by conventional methods (top), and if fluidized bed impregnation is introduced (bottom).

[Color figure can be viewed in the online issue, which is available at wileyonlinelibrary.com.]

unchanged, which is advantageous for powder flow, (2) size segregation of excipient and API particles is eliminated, which has a beneficial effect on blend uniformity, (3) final properties of impregnated materials are governed almost exclusively by the physical properties of the excipient, (4) release kinetics of poorly soluble API could be improved by using highly porous excipients with small pore size, which will increases the effective surface area for dissolution, (5) release kinetics could also be controlled by coimpregnation of API and appropriate polymers, (6) API physical properties control becomes unnecessary since the API particles are formed during impregnation, (7) introduction of additional excipients to modify the flow of final product is no longer needed, and (8) elimination of several unit operations from drug substance and drug product development is facilitated, as is depicted in Figure 1

Materials, Equipment and Methods

Materials

For any impregnation process to be commercially viable, a special consideration needs to be taken when choosing the excipient. The ideal excipient candidate for impregnation should have the following properties (1) to be a common and widely available excipient such as a filler or a diluent (not lubricants and glidants), (2) to have good flowability, (3) to have a narrow particle-size distribution (PSD), (4) to be insoluble in a variety of organic solvents to minimize dissolution and granulation during impregnation, (5) to be physically stable under FB conditions (stable physical form, mechanically stable), and (6) to be porous—to possess high-internal surface area, the most important property for successful impregnation. Three common excipients were initially considered for this study (Figure 2). Spray-dried lactose (fast flow) possesses good flowability, poor solubility in some solvents, and can be obtained with narrow particle-size distribution, however, it is not in stable form (amorphous) and not very porous (SSA of 0.18 m^2/g by BET). Similarly, Avicel® 102 has good flowability, it is nonsoluble in most solvents and has a stable physical form. However, it has low-surface area (SSA of 0.89 m^2/g by BET), and wide particle-size distribution. The excipient which was chosen for impregnation was anhydrous dibasic calcium phosphate ($CaHPO_4$). It has excellent flowability, it is nonsoluble in organic solvents, it has a stable physical form[28] and a narrow particle-size distribution. Most importantly, it has a high-surface area of 15.34 m^2/g by BET.

Anhydrous dibasic calcium phosphate (Anhydrous Emcompress®, purity 98–103%) was purchased from JRS Pharma LP (Patterson, NJ USA). Methanol, B&J Brand® Multipurpose Grade (purity above 99%), was purchased from VWR International. Acetaminophen (APAP, purity 99–101%)

micrometerized was purchased from Mallinckrodt, Inc. (Raleigh, NC, USA). Gelatin capsules (100% gelatin, size 1, Coni-Snap) were purchased from Capsugel®.

Equipment

All impregnation experiments were carried out in a GLATT GPCG 1 fluidized-bed dryer/coater/granulator, equipped with a top spray nozzle. Impregnated material was milled using a 2″ laboratory scale pin mill, LPM-2 (Hosokawa Micron Powder Systems). Capsules were prepared using semiautomatic capsule filling mashie (CAP 8) by Capsugel®. Individual tablets were prepared using Presster™, a tablet press replicator and compaction simulator sold by MCC (East Hanover, NJ USA).

Experimental Setup and Procedure

Experimental setup

A diagram of our fluidized-bed impregnation equipment setup is shown in Figure 3 The system consists of a Glatt GPCG1 fluidized-bed dryer equipped with top spray nozzle and peristaltic pump connected to two holding vessels via a three-way valve. One of the vessels is used to hold pure solvent and the other, which is placed on a scale, is used to hold the APAP solution. The scale is used to monitor the solvent/solution spray rate or total API uptake into the excipient. The spray nozzle is positioned in such a way that allows it to be immersed inside the fluidized bed during impregnation. Having the nozzle just below the surface of the fluidized bed is important to minimize spray drying of the droplets and ensure impregnation of the solution into the excipient before drying. Important setup parameters before impregnation are drying gas inlet velocity (or flow rate), drying gas inlet temperature and atomization gas pressure. Important parameters monitored during the impregnation process are product temperature, solution/solvent spray rate and pressure drop across top filter element (indicates when shaking of the filter element is required).

Experimental procedures

Impregnation. The procedure developed for the fluidized-bed impregnation of excipients consists of the following several steps:

1. Charge fluidized-bed dryer with excipient until the top spray nozzle is reached. During fluidization, the nozzle needs to be located within the bed to minimize spray drying.
2. Start fluidized-bed dryer and set the inlet gas temperature to desired value.
3. Begin spraying pure solvent. Continue spraying until steady state is achieved (constant product temperature).
4. Once steady state is achieved, begin spraying API solution. Continue spraying until desired loading is achieved.
5. Switch back to spraying pure solvent for specific time.
6. Dry product for specified time, cool down and unload.

Three impregnation studies involving APAP and $CaHPO_4$ are presented in this study. The aim of these studies was to achieve three different weight percent's of APAP loading within the excipient: medium (9–10%), low (0.9–1.0%) and ultra-low (0.09–0.1%). All of these experiments were executed following the above procedure. Details on the experiments in terms of amounts of APAP and excipient, concentration of APAP solution, spray time and processing parameters, such as inlet and product temperatures, are given in Table 1.

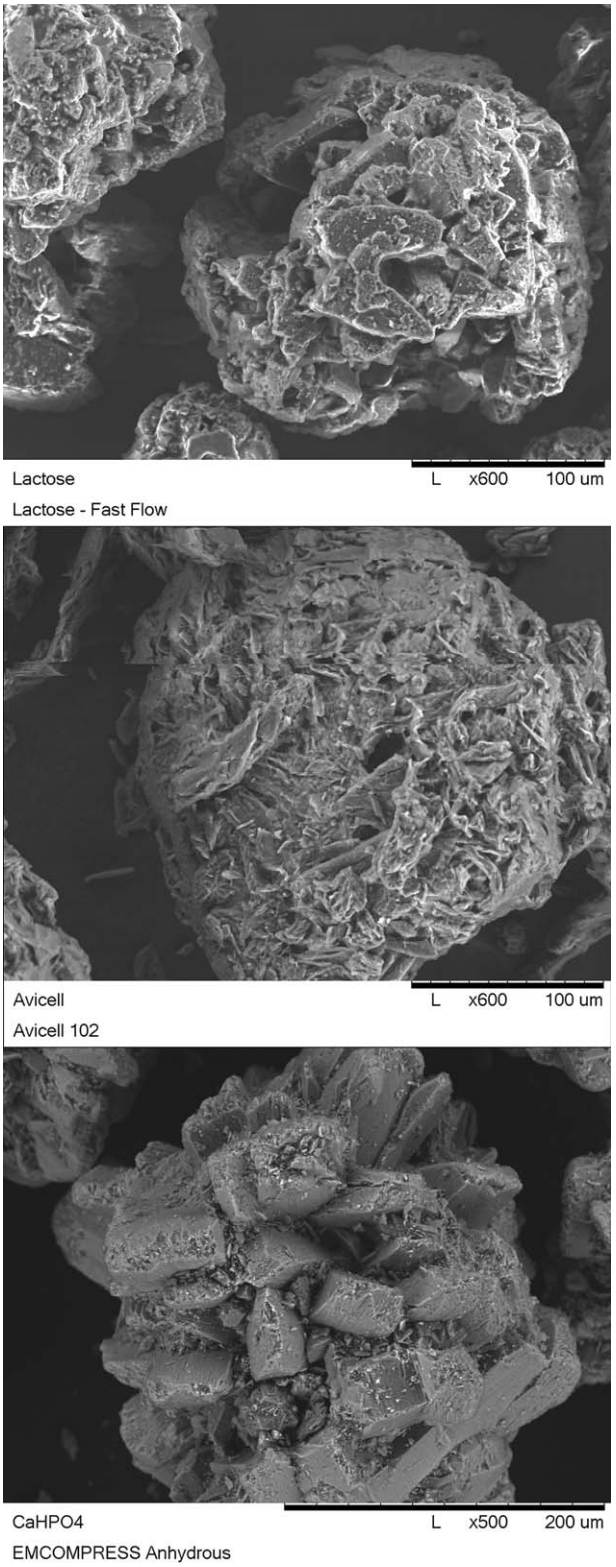

Figure 2. SEM pictures of lactose-fast flow (top), Avicel® 102 (middle) and anhydrous $CaHPO_4$ (bottom).

All experimental conditions were kept constant with the exception of the APAP solution concentration, which was varied accordingly to achieve the target loading. Spraying

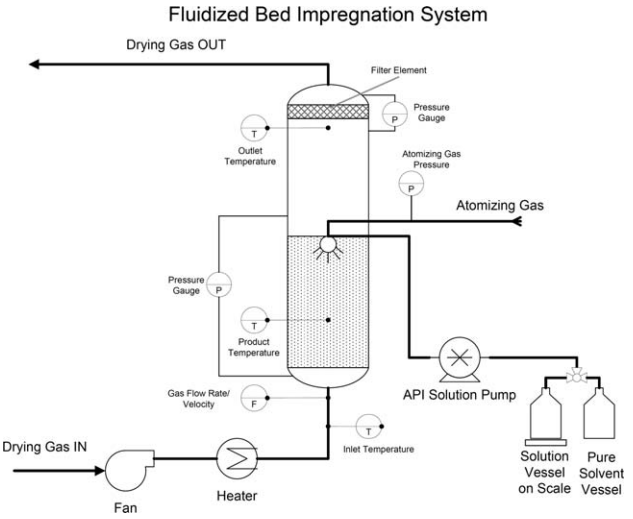

Figure 3. Fluidized-bed impregnation system setup.

pure solvent after the APAP solution is an important part of the impregnation procedure, as it allows for any amounts of deposited APAP on the surface of the particles to be redissolved and deposited within the excipient. At the end of each experiment, the impregnated material was dried until product temperature reached 60°C, after which the heat was turned off and contents of the fluidized bed were cooled down to room temperature.

Milling. Milling of the impregnated materials was performed on a 2″ laboratory scale pin mill. The material was fed to the mill using a vibratory feeder. Feed rate used was around 10 g/min. Mill speed used was 10,000 rpm.

Capsule Filling. Capsule filling was performed on a semiautomatic CAP 8 machine. Equipment settings used during filling were: 90° auger, rotary table at maximum speed, rectifier at maximum speed. Two batches of 450 capsules were filled with each material. Only the second batch was used for blend uniformity and dissolution analysis.

Analytical Methods

The following analytical methods were employed to complete the physical characterization of impregnated and pure $CaHPO_4$.

Microscopy. All pictures were made using a Hitachi table-top scanning electron microscope TM-1000.

Particle-Size Distribution (PSD). Particle-size distributions of all materials were analyzed using Beckman Coulter LS 13320 laser diffraction particle size analyzer.

Specific Surface Area (SSA) and Pore-Size Distribution. Specific surface area (in m^2/g) was determined by the BET standard method (5-point N_2 adsorption). Cumulative pore-size distribution (in cm^3/g) was determined using the BJH adsorption isotherm (42-point N_2 adsorption). All nitrogen adsorption measurements were recorded at −196°C on a TriStar® 3000 instrument (micromeritics). All samples were degassed for at least 18 h at 30°C before measurement.

Drug Loading and Blend Uniformity. Drug loading and blend uniformity analysis was determined by HPLC analysis of representative samples using Waters 2695 HPLC System. Details on the method used for quantification of acetaminophen are as follows: column – Aqua 5 μm C18, 150 × 4.6 mm; mobile phase—water/methanol/acetic acid (69:28:3); flow rate – 1.5 mL/min; UV detection – 275 nm.

Determination of drug loading across various particle size ranges and as an average was performed by first sieving impregnated $CaHPO_4$ and determining the weight fraction of each size range. Samples of each size range (between 400 to 800 mg, depending on estimated loading) were weighted out in a 50 mL volumetric flask which then was filled with methanol to the mark. The $CaHPO_4$/methanol mixture was then sonicated in a sonication bath for about 40 min to ensure full acetaminophen dissolution. Flasks were left overnight to equilibrate at room temperature and to allow solid contents to settle. Samples from the supernatant were then filtered through 0.45 μm syringe filters and placed in HPLC vials for analysis. To quantify the API content, three sets of two standard solutions of APAP in methanol(one set for each lot of impregnated $CaHPO_4$) were also prepared with concentrations slightly below and slightly above of the samples to be analyzed. Using the two standard solutions, a three-point calibration curves (including zero as third point) were generated (R^2 above 0.9998) and used in all calculations. Injection volume for each test run was 10 μL. Two injections were run for each sample and the average was used for calculations. After determining the APAP loading for each size fraction, average loading corresponding to the whole impregnated lot was calculated using already predetermined weight fractions.

Determination of blend uniformity was performed by analyzing individual capsules filled with impregnated $CaHPO_4$ for APAP loading. Ten capsules were randomly chosen from each impregnated lot (ca. 450 capsules per lot) and their contents were placed in 50 mL volumetric flasks, which were then filled with methanol. Weight of impregnated $CaHPO_4$ in the gelatin capsules was in the range of 500–550 mg. Contents of the flasks were sonicated for about 40 min and then left overnight to equilibrate at room temperature and for contents to settle. Samples from the supernatant were then filtered through 0.45 μm syringe filters and placed in HPLC vials for analysis. To quantify the API content, three sets of two standard solutions of APAP in methanol (one set for each lot of impregnated $CaHPO_4$) were also prepared with concentrations slightly below and slightly above those of the samples to be analyzed. Using the two standard solutions, a three-point calibration curves (including zero as third point) were generated (R^2 above 0.9998) and used in all calculations. Injection volume for each test run was 10 μL. Two injections were run for each samples and the average was used for calculations. After calculating the drug

Table 1. Experimental Conditions, Process Parameters and Corresponding APAP Loading for Three Different Impregnation Experiments in Fluidized Bed

	#1	#2	#3
Weight of $CaHPO_4$, g	3900	3900	3900
APAP Solution Concentration, mg/ml	128.15	14.40	1.44
Spray Rate, ml/min	17	17	17
Spray Time, min	160	160	160
Inlet Gas Velocity, m/s	1.3–1.5	1.3–1.5	1.3–1.5
Atomization Pressure, bar	2	2	2
Inlet Temperature, °C	85	85	85
Product Temperature, °C	43–45	43–45	43–45
Achieved Loading, % w(API)/ w(pure $CaHPO_4$)	8.87	0.99	0.1

loading for each capsule, the mean, the standard deviation and the % relative standard deviation (% RSD) were calculated accordingly.

Differential Scanning Calorimetry (DSC). To study the physical state of APAP in the porous matrix of anhydrous $CaHPO_4$, the loaded powders were analyzed using a differential scanning calorimeter Q100 by TA Instruments. The samples were heated from room temperature to 210°C with a 10°C/min heating rate. All samples (weight range of 20–30 mg) were analyzed in a pin-hole aluminum sample pans.

Powder X-Ray diffraction (pXRD). Powder diffraction data was obtained using a LabX XRD-6000 X-ray diffractometer (Shimadzu) with a graphite monochromator and diffracted beam generated by Cu tube. The pXRD patterns were collected with 40 kV of tube voltage and 30 mA of tube current in the angular range (2θ) of 10–50° in a continuous scan mode with a scanning speed of 0.5 deg/min.

Bulk/Tapped densities. Bulk density was determined using the FT4 powder rheometer from Freeman Technology. This method minimizes inconsistencies often observed in other approaches due to uneven filling of the measuring vessel, where variations in filling techniques can lead to variations in packing, which in turn will lead to variations in measured bulk density. Therefore, to achieve good reproducibility it is essential to measure the density of the powder in relation to a known and controlled packing state. The FT4 allows for the powder to be conditioned and to establish a homogeneous packing state with low stress. After the conditioning cycle, the powder sample is free of localized stress and excess air. This process is automated and is independent of the operator. As a result, the FT4 yields a very reproducible packing state and allows the user to calculate a very reproducible bulk density. The tapped density was measured using a 100 mL graduated cylinder (filled to the 90 mL mark with powder) and a bench-top tapped density meter. Tapped density was measured using a total of 1,250 taps, a point after which no change in volume was visually detected.

Dissolution Testing. To study dissolution and release of APAP from impregnated $CaHPO_4$, the filled gelatin capsules were analyzed using Varian's Vankel VK-7010, 8-spindle, 8-vessel USP dissolution apparatus with automated online UV–vis measurement. The specific method employed in the analysis was implemented in accordance with the USP Apparatus I (basket) method. Additional details on the dissolution analysis include: dissolution media – 900 mL phosphate buffer at pH = 5.8; agitation speed – 100 rpm; UV detection – 243 nm. To determine the amount of APAP, each filled capsule was weighted before testing and the average weight of a pool of empty capsules was subtracted to give the amount of impregnated powder inside the capsule. Knowing the filled weight and the average APAP loading for the specific impregnated lot, the average amount of drug was calculated. The average weight of the empty capsules was determined by randomly weighing 50 empty gelatin capsules and it was determined to be 72.81 mg (% RSD = 1.15%). Only impregnated powders with 1% loading and above were analyzed due to the limit of detection of the instrument. The amount of impregnated powder inside the capsules ranged between 500 and 550 mg. To quantify the analysis, a calibration curve was constructed ($Abs = 59.39067^{*}Conc + 0.04196$, $R^2 = 0.99762$) and used over the concentration interval of the experiments. A total of six capsules were tested from each material and results were then averaged.

Tableting and Compressibility Testing. Individual tablets of pure $CaHPO_4$, impregnated $CaHPO_4$ (1 and 9% loadings) and physical blends of APAP and $CaHPO_4$ (7.25% and 14.00%) were made using the Presster™, a tablet press replicator and compaction simulator. Initial sets of experiments were carried out for each powder to determine the dosing position on the equipment necessary to produce tablets with identical weight (0.92 g). After all settings were determined, a set of 10 tablets was produced from each powder by varying only the compression position (4.25–6.25 mm), which directly correlates to different compression force (8–37 kN). The thickness of each tablet was measured with a caliper. The hardness of each tablet was determined using bench-top hardness tester (model 6D, Dr. Schleuniger® Pharmatron). All tablets were produced without any additives. Tableting of pure CaHPO4 without any additives proved to be difficult as all tablets exhibited partial capping during ejection. Only the tablet thickness of the pure excipient tablets was measured when possible (where the two faces of the tablets were still partially available).

Shear Cell Testing. Rotational shear testing was performed using the FT4 powder rheometer. A detailed description of the shear testing method can be found in Freeman et al.[30] First, the powder is conditioned by passing a rotating blade through the bed to achieve a homogeneous reproducible state. Then, the powder bed is slowly precompacted by applying the pre-shear normal load with a vented piston to displace the entrapped air. This consolidated sample is presheared (15 kPa normal stress) to achieve an overconsolidated state (until the shear stress reaches a steady state at the pre-shear normal stress). After the steady state is achieved, the normal stress is lowered to the maximum value required for the actual measurements (9 kPa normal stress), and the sample is sheared further to obtain a yield point. The preshear/shear sequence is repeated for a total of 5 times to obtain a yield locus.[29] For each material (pure and impregnated), the yield loci were obtained at only 9 kPa of normal stress and each yield locus was examined using Mohr stress circle analysis to obtain the values of major principal stress, unconfined yield strength and cohesion.[29,30]

Results and Discussion

Proof of impregnation

There are three possible outcomes of the proposed fluidized-bed process, with only one (impregnation) being the desired one. The two undesired outcomes are spray drying of the API and spray coating of the excipient. In this section, we focus our attention on the question "Was the excipient impregnated?" This issue is examined by conducting three types of physical analysis on the impregnated blends: scanning electron microscopy, specific surface area and pore-size distribution and finally, by testing the drug loading.

Spray drying of the API is easily ruled out by HPLC analysis on the impregnated materials, which is performed to determine the final drug loading (see complete details in the section "Drug loading and blend uniformity"). The loading of the API, as discussed later, was determined for various particle size fractions (obtained by mechanically sieving the powders) and then averaged. In the event that the API was

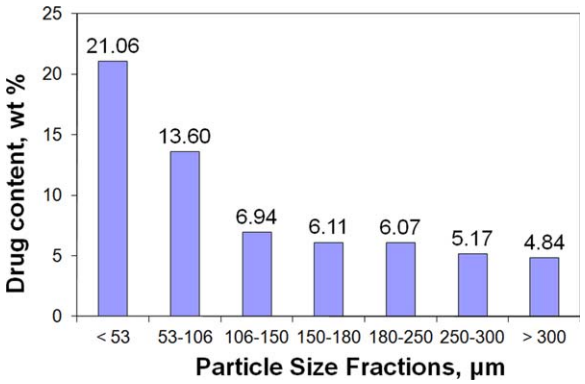

Figure 4. APAP weight fraction (wt. APAP/wt. $CaHPO_4$) across different size fractions for 8.87% average loading.

[Color figure can be viewed in the online issue, which is available at wileyonlinelibrary.com.]

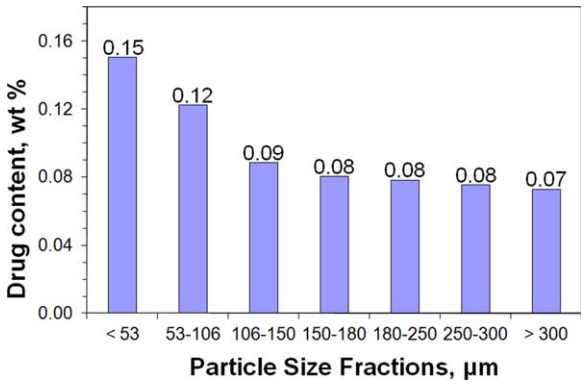

Figure 6. APAP weight fraction (wt. APAP/wt. $CaHPO_4$) across different size fractions for 0.10% average loading.

[Color figure can be viewed in the online issue, which is available at wileyonlinelibrary.com.]

spray dried, three possible outcomes could be observed: (1) collecting all the spray-dried API with the smallest particle size fraction (<53 μm) during sieving (the size of droplets produced, hence, final API particles, are on average less than 20 μm due to the nozzle and atomization pressure used during impregnation). (2) Losing most (or all) of the spray dried API through the outlet filter, which has size of about 50 μm. (3) Having spray-dried API particles attached to the surface of the carrier. If scenario (1) was true, then all of the API must show with the lowest size fraction (<53 μm) with almost no API in the upper fractions. If scenario (2) was true, then the amount of API analyzed should be considerably lower than the target loading (or even zero). If scenario (3) was true, then there should be clear evidence in the SEM pictures of excipient particles attached to spherical API particles (spherical because of API spray-drying). Neither the first nor the second scenarios take place, as it is evident from Figure 4, Figure 5 and Figure 6. All size fractions receive appropriate amounts of API (see explanation in the section "Drug loading and blend uniformity") and the average loading (calculated based on data in Figure 4, Figure 5, Figure 6 and Table 2) is consistent with the total sprayed amount of API during processing (see data in Table 1). There is no loss of API and all of it is distributed throughout the excipient. The third scenario is examined by analyzing SEM pictures of impregnated $CaHPO_4$ (Figure 7), which clearly show that this last scenario does not occur either. Therefore, spray drying of API solution during fluidized-bed impregnation process can be ruled out with a high level of confidence.

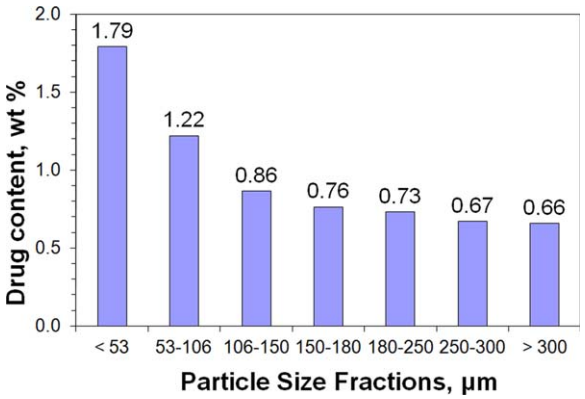

Figure 5. APAP weight fraction (wt. APAP/wt. $CaHPO_4$) across different size fractions for 0.99% average loading.

[Color figure can be viewed in the online issue, which is available at wileyonlinelibrary.com.]

Spray coating is the second undesired outcome during the impregnation process. As it was described in the section "Materials, Equipment and Methods", the process parameters (product temperature, inlet temperature) and the overall procedure are chosen carefully to promote impregnation and suppress coating. To rule out spray coating, we first examine all impregnated powders under the microscope. Figure 7 shows SEM pictures of various size fractions of impregnated $CaHPO_4$ along with pure $CaHPO_4$. Thorough examination of all pictures (full set of pictures not shown) did not yield any visual sign of coating. All impregnated particles look almost identical to pure $CaHPO_4$. In the event of coating, the rough surface of the particles should have been smoothed and gaps and crevices filled up by the applied layer of API.

Although SEM pictures demonstrate absence of spray drying and surface coating, to firmly establish the proof of impregnation, all powders (impregnated and pure) were further tested for their total surface area and pore-size distributions. A relatively porous material, in theory, should possess high-total surface area, in the order of few an m^2/g as a minimum. On the contrary, a completely nonporous material with particles of several micrometers usually has total surface area below 1 m^2/g. Simple calculation shows that for uniformly distributed spheres, 2 μm in diameter with a true density of 2.96 g/mL (true density of $CaHPO_4$ anhydrous,[31]

Table 2. Weight Fraction for all Particle Size Groups in Impregnated $CaHPO_4$, Runs 1, 2 and 3

	Weight Fraction, %		
Particle Size Fraction, μm	Run #1	Run #2	Run #3
below 53	1.65	10.42	11.25
53–106	32.57	25.16	24.29
106–150	13.19	17.36	19.54
150–180	6.80	12.90	16.58
180–250	43.86	32.41	26.78
250–300	1.35	1.05	1.05
above 300	0.58	0.69	0.51

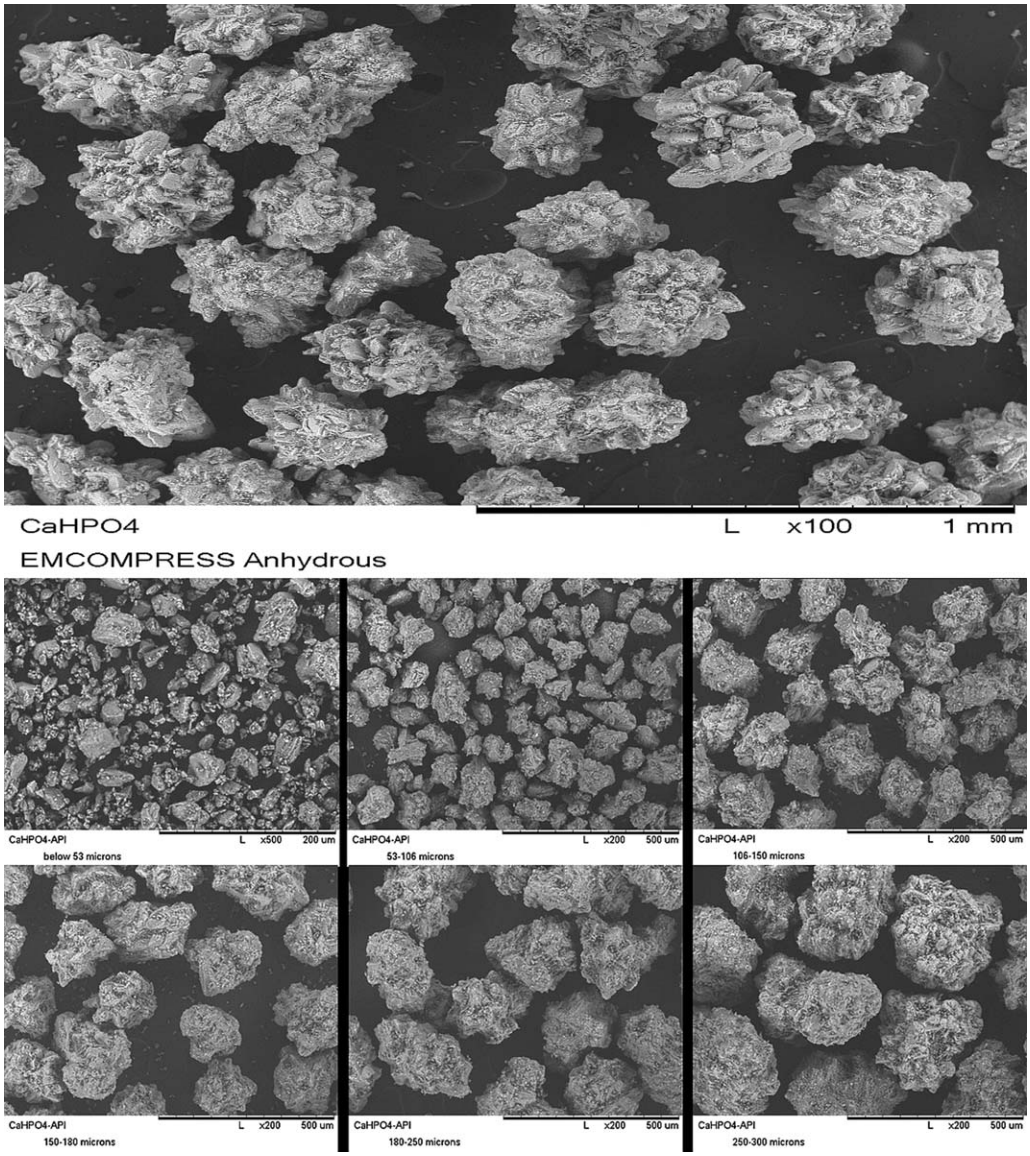

Figure 7. SEM pictures of pure (top) and various size fractions of impregnated (bottom, 8.87% loading) $CaHPO_4$.

the total surface area should be around 0.5 m^2/g. Therefore, examining and comparing changes in specific surface area and pore size distribution for pure and impregnated $CaHPO_4$ should give a useful indication of impregnation vs. coating. In the case of spray coating, which requires the drying process to be much faster than impregnation, all particles would receive a layer of (most likely amorphous) API. This layer would block the internal surface of the particles from the N_2 gas during surface area measurements and the corresponding SSA would be comparable to that of a nonporous material.

However, this is not the case as it is evident from Figure 8 and Table 3, which summarize SSA and pore-size distribution measurements for pure and impregnated $CaHPO_4$ (8.87% and 0.99% loading). Measurements for the lowest loading of 0.1% were performed but not included since they did not show any difference compared to pure excipient. For each size fraction shown on the figure, we observe a decrease in SSA and total pore volume (for micropores and mesopores with $d_{pore} < 120$ nm) proportional to the level of loading (see section "Drug loading and blend uniformity" for discussion on loading). In neither case do we detect SSA values indicating spray coating of particles. Even for the size fraction with the highest loading (<53 μm, Table 3) there is still high-residual porosity, as indicated by the corresponding SSA of 6.3 m^2/g. Therefore, from all these data, it can be concluded with significant confidence that the carrier particles are impregnated and that spray coating is not evident. The proposed FB impregnation process does indeed promote impregnation of particles when process conditions are chosen carefully.

Drug loading and blend uniformity

It was shown already (Table 3) that variations in the API uptake by different size fractions of the excipient were observed during impregnation (as indicated by differences in surface area and pore volume at the end of impregnation). To better assess the drug loading, the final product was sieved and HPLC analysis was performed on each fraction. The results are shown in Figures 4, 5 and 6. The average loading was calculated based on these results and on the

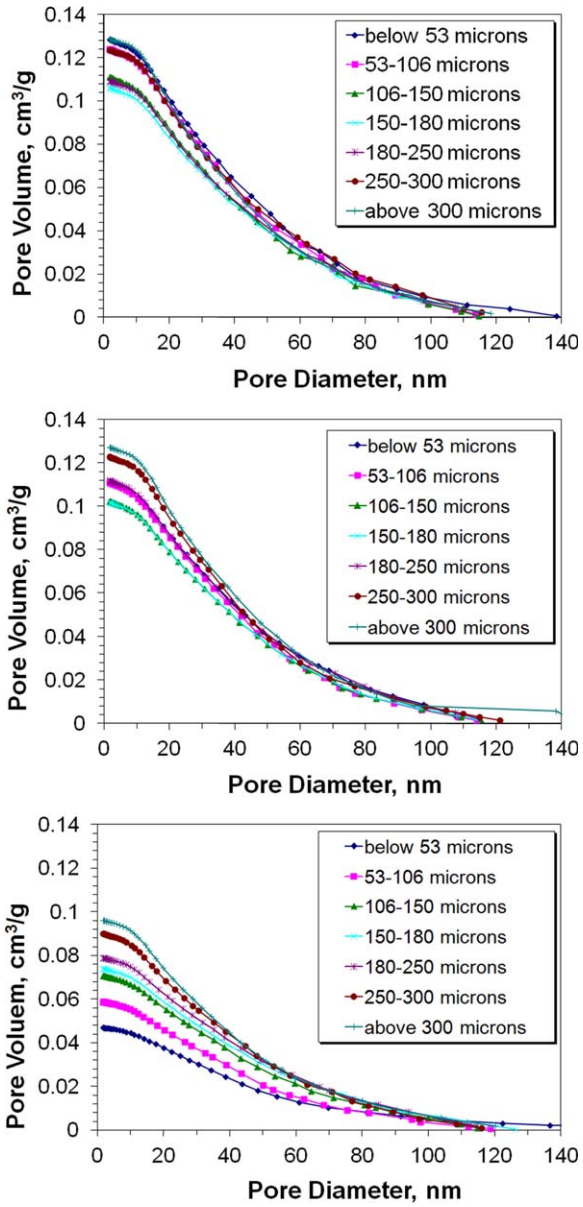

Figure 8. Cumulative pore-size distributions (for pores with $d_{pore} < 120$ nm) for various sieved fractions of pure (top), and impregnated $CaHPO_4$ (middle – 0.99%, bottom – 8.87%).

[Color figure can be viewed in the online issue, which is available at wileyonlinelibrary.com.]

mass fractions of each size group in the blend, data shown in Table 2. There is an emerging pattern, characteristic for all three materials—the API loading is inversely related to the size of the particles being impregnated. This is not surprising and can be explained in terms of the flux of API solution across the external surface (not to be mistaken with total surface area, which also includes internal surface area) of the particles. During fluid bed impregnation, this flux is constant for all size particles if one assumes a well-mixed system. The difference comes from the fact that particles of pure $CaHPO_4$ (as in any other powder) have a PSD, which in mathematical terms translates to differences in the external surface-to-volume (or surface-to-mass) ratio of different size particles. Therefore, a constant flux of material causes particles with high surface-to-volume ratio (i.e., smaller particles) to receive a larger mass fraction of solution for a given time.

From these data it can be concluded that the PSD of the excipient is an important characteristic, which determines the final drug loading (or variation thereof) during FB impregnation. Having a porous carrier with a narrower PSD will result in less variation in the drug loading across size groups. It will also allow for higher drug loadings to be achieved. For example, Figure 4 shows that for the size group of "below 53 μm" the loading is 21.06%, when the average loading is only 8.87%. A narrower PSD allows achieving the highest loading possible without overfilling the smallest size particles. This highest theoretical loading will depends on the porosity of the excipient and the true densities of the API and excipient.

Any given pharmaceutical formulation has to be assessed in terms of its blend uniformity—that is how well the API is dispersed throughout the excipient. The blend uniformity for the impregnated materials presented in this study was assessed by first formulating them into hard gelatin capsules without any other additives. These capsules (having around 0.50–0.55 g of impregnated powder) were then taken and 10 of them were randomly chosen for HPLC analysis. The absolute amount of API in each capsule was determined and its concentration (in terms of weight %) calculated. The blend uniformity was calculated as % relative standard deviation (%RSD) from the mean value of the concentration. The results from this analysis for all three impregnated materials are presented in Table 4 along with the capsule weight variability (measured on 50 randomly chosen capsules). Drug content uniformity (also presented) was calculated as % relative standard deviation from the mean value of the API's absolute amount in each capsule. All results for blend uniformity are around 1% RSD or less which indicates a highly uniform pharmaceutical blend. There are larger variations in drug content uniformity which are primarily due to the capsule weight variability.

In general, highly uniform blends are difficult to achieve, especially when working with low-drug loadings. This is

Table 3. Total Surface Area and Total Pore Volume (for Pores with $d_{pore} < 120$ nm) for Various Sieved Fractions of Pure and Impregnated $CaHPO_4$

	BET Surface Area, m^2/g			Total Pore Volume, ml/g		
Particle size, μm	Pure CaHPO4	Impregnated, 8.87%	Impregnated, 0.99%	Pure $CaHPO_4$	Impregnated, 8.87%	Impregnated, 0.99%
below 53	17.9961	6.3476	15.5627	0.1227	0.0449	0.1029
53–106	17.5024	8.2280	16.1061	0.1177	0.0554	0.1049
106–150	15.9307	9.8040	14.8991	0.1053	0.0657	0.0963
150–180	15.3127	10.1691	14.7922	0.0989	0.0683	0.0952
180–250	15.5947	10.8102	15.3162	0.1022	0.0742	0.1050
250–300	17.2800	13.3033	18.1248	0.1141	0.0850	0.1184
above 300	18.6128	13.5981	18.3431	0.1210	0.0909	0.1218

Table 4. Blend Uniformity, Capsule Total Weight Variability and Drug Content Uniformity of Capsules Filled with Unmilled $CaHPO_4$, Impregnated to Different Levels of APAP

APAP Loading, % (wt APAP/wt pure $CaHPO_4$)	Blend Uniformity, %RSD	Capsule Total Weight Variability, %RSD	Drug Content Uniformity, %RSD
8.87%, un-milled	1.05	2	1.73
0.99%, un-milled	0.7	1.52	1.18
0.01%, un-milled	0.99	0.79	1.01

primarily due to inadequate mixing of the ingredients and size segregation of the particles (API and excipient). In such cases, conventional formulation techniques call for additional unit operations, such as wet or dry granulation, to help achieve targeted blend uniformity. What we have shown here are highly uniform blends, achieved with a single-unit operation without any special control of API physical properties. The API (and its physical properties) does not play a role in determining the uniformity of the blend, as it is located inside the excipient particles. However, there is still a chance for size segregation due to the inherent PSD of the excipient particles. As we have shown already, various size groups have different drug loadings and if they are segregated, they will affect the final blend uniformity. To further improve homogeneity of the impregnated materials we examined the effects of size reduction. Milling of the impregnated powders was done on a laboratory scale pin mill using mild conditions (low range of milling speeds). The resulting powders were used again to fill hard gelatin capsules and then tested by HPLC for drug content. All blend uniformity results on the milled materials are summarized in Table 5. Particle-size distributions are discussed in one of the next sections. For all three impregnated materials, there was further improvement of blend uniformity, which in some cases led to reductions in the RSD of 50% or more. Again, variation in drug content uniformity is mainly due to the weight variability of the filled capsules. The variability of the filled capsule's weight is primarily due to the semiautomatic fashion in which they were filled (variation between experiments such as hopper fill level). These results underline the importance of the PSD of the excipient being impregnated. Using an excipient with narrow PSD will allow not only higher drug loading but also a more uniform dispersion of the API.

Physical state of the drug molecules inside the carrier

The proposed impregnation method could be viewed as a slow evaporative process during which the API precipitates/crystallizes out of solution as it is being deposited within the mesoporous and microporous structure of the excipient. The question that remains is in what physical form the drug molecules are deposited inside the carrier? There are three possible outcomes: crystalline material, amorphous material or molecular dispersions. Factors that determine the actual physical form of the impregnated drug include: the nature of the API (some form amorphous state easier than others), the solvent system and the internal structure of carrier matrix (pore size and distribution). Whether crystalline or amorphous material is deposited will depend on the first two factors while the formation of a molecular dispersion will be influenced by the third one. Solid molecular dispersion is a state of matter, similar to amorphous, in which the intermolecular interactions are broken-up and the molecules are individually separated and dispersed throughout the pores. This scenario is possible since equilibrium thermodynamics predict that crystallization should be completely suppressed below a certain critical pore diameter d_{cr}. Surface energy contributions in this case over-compensate the energy advantage associated with crystallization. The critical diameter d_{cr} typically amounts to a few nanometers.[14] In larger size pores the state of matter will be either amorphous or crystalline, depending on the nature of the API, solvent or processing conditions. It is possible by controlling the pore size to prevent the crystallization of the amorphous material,[14] or to preferentially obtain one crystal form vs. another.[21] In all cases there will be a shift of the bulk API's melting point to lower values depending on the size of the pores. This is due to the well-known phenomenon of confinement-induced melting point depression. The new melting point can be estimated using the Gibbs-Thompson equation of the form[32]

$$T_m(\mathrm{d}) = T_m^{\infty} - 4\sigma_{\mathrm{s1}} T_m^{\infty} (\mathrm{d_p} \Delta H_{\mathrm{m}\rho\mathrm{c}}) \quad (1)$$

where $T_m(\mathrm{d})$ is the depressed melting point for pores with diameter d, T_m^{∞} is the bulk melting point, σ_{sl} is the surface tension between crystal and liquid phases, ΔH_m is the heat of melting, and ρ_c is the bulk density of the solid phase.

Differential scanning calorimetry (DSC) is a very powerful analytical tool used to investigate the physical state of solids. In the case of amorphous material, DSC will show an exothermic peak due to crystallization of the solid followed by an endothermic peak due to melting of the crystalline solid. When only a crystalline material is present, the exothermic peak (amorphous) will be absent. If the crystalline solid is confined to small pores (as it was explained already) there will be a shift of the melting peak to a lower value. In the case of a molecular dispersion there will not be any visible endotherm or exotherm peaks.

All three impregnated materials were analyzed using DSC, however only the ones with 8.87% and 0.99% loadings are

Table 5. Blend Uniformity, Capsule Total Weight Variability and Drug Content Uniformity of Capsules Filled with Milled $CaHPO_4$, Impregnated to Different Levels of APAP

APAP Loading, % (wt APAP/wt pure $CaHPO_4$)	Blend Uniformity, %RSD	Capsule Total Weight Variability, %RSD	Drug Content Uniformity, %RSD
8.87%, milled	0.54	1.19	1.65
0.99%, milled	0.56	1.73	1.91
0.01%, milled	0.42	2.25	2.79

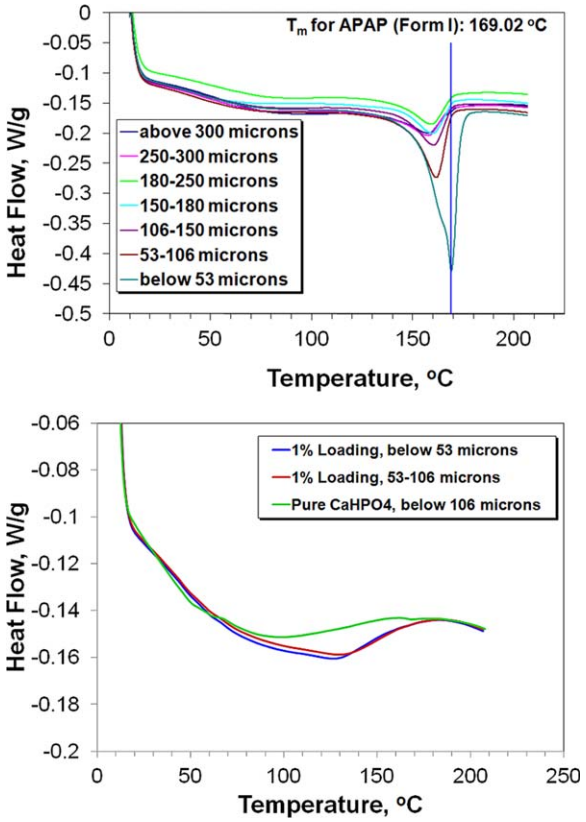

Figure 9. DSC test results: Top – $CaHPO_4$ impregnated to 8.87% loading; Bottom – $CaHPO_4$ impregnated to 1% loading and pure $CaHPO_4$.

[Color figure can be viewed in the online issue, which is available at wileyonlinelibrary.com.]

presented here (see Figure 9). The DSC scans for 0.1% impregnated material did not show any thermal events, most likely due to the fact that the actual API amount in the DSC scans was below the limit of detection for this analytical technique. In the case of 8.87% loading (Figure 9, top), the amount of impregnated API was enough to give a very clear DSC signal with high intensity. Due to the difference in APAP loading, DSC scans of all size groups were taken. For all size groups there is a clear shift in the melting point of APAP from its bulk melting point of 169.02°C (form I). This is a clear indication of the small confinement of APAP molecules, which is another proof of impregnation. These melting point shifts are within a temperature range of 150–170°C, well in agreement with already evaluated shifts for APAP form I in pore sizes ranging from 20 to 100 nm.[21] All melting peaks show some broadening as well due to the inherent pore-size distribution within the excipient. The melting peak for the size group of 53 μm and below shows some overlap with the bulk melting point. This could be an indication of complete filling up of the macropores (d_{pore} >120 nm), which as suggested by[18] in the case of $CaHPO_4$ granules and Ibuprofen, is about 22%. In the case of 0.99% loading (Figure 9, bottom), the amount of impregnated API was at the borderline of limit of detection for the DSC instrument. Therefore, only the size fractions with the highest loadings are presented along with a scan for the pure $CaHPO_4$ excipient. The pattern is the same as outlined above (broadening and shifting to lower temperatures) although it is clear that the peaks are weaker, getting near the limit of detection. Sensitivity of the DSC technique (along with the actual API loading) should be considered if it will be used to characterize impregnated materials.

Figure 10 shows the differential pore-size distribution for the same material (8.87% loading). From these data it can be confirmed that most of the impregnation is taking place with the pore-size range of 10–100 nm, as was suggested earlier. There might be some small amount of APAP in smaller pores (<5 nm) in the form of molecular dispersion as suggested from the same plot. Powder XRD analysis was also performed to confirm the physical form of impregnated $CaHPO_4$. Tests were performed only on the high-loaded material due to detection limitations associated with this technique. Figure 11 shows XRD scans for various size groups and for pure $CaHPO_4$ and pure APAP form I as comparison. The figure does not show the full range of scans (2θ of 10–50°) for the sake of clarity. Acetaminophen Form I can be confirmed by several peaks around 2θ of 15–25°.

Overall Physical Properties of the Impregnated Excipient

Particle-size distribution

Every excipient is friable to some degree. For the FB impregnation method to be commercially viable, it must be able to preserve the original physical properties of the excipient almost unchanged. Therefore, an important question to be answered is how the particle size changes due to the continuous fluidization during the impregnation process. Total fluidization time in all of the experiments, which includes impregnation time plus the initial startup and final drying, was in the order of 4 h. Particle-size distribution data for pure $CaHPO_4$ and for various impregnated $CaHPO_4$ lots is shown on Figure 12 Comparing PSD data for pure and impregnated samples (unmilled) proves that the changes in size are not significant. There is some small amount of fines generated due to attrition that takes place during the process. Additional, more detailed experiments are needed to determine if these fines are generated constantly throughout the process or only at the beginning of the fluidization, when the particles are still dry and not loaded with API. It could be argued that having a drug impregnated within, could further mechanically stabilize the particles (see section &;dquo;Tableting and compressibility study").

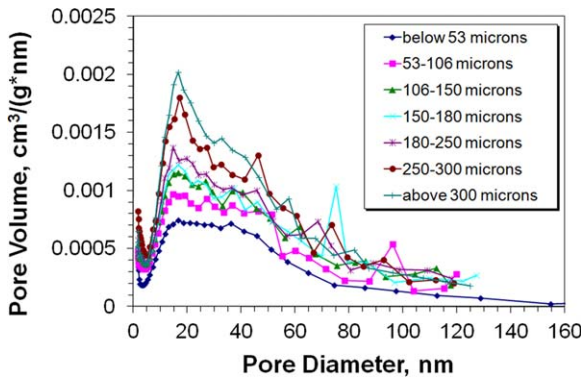

Figure 10. Differential pore volume distribution for various size fractions of impregnated $CaHPO_4$ with APAP to 8.87% loading.

[Color figure can be viewed in the online issue, which is available at wileyonlinelibrary.com.]

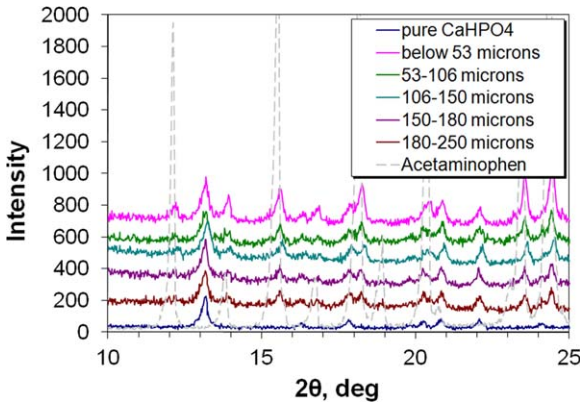

Figure 11. XRD pattern comparison between pure $CaHPO_4$, various size fractions of impregnated $CaHPO_4$ (8.87% loading) and pure APAP.

[Color figure can be viewed in the online issue, which is available at wileyonlinelibrary.com.]

Figure 12 also compares PSDs of impregnated $CaHPO_4$ before and after milling. As it was shown in section "Drug loading and blend uniformity", milling was used to further improve blend uniformity of the impregnated materials. One way of explaining this experimental fact, as it is evident from the PSD data, is that reduction in size of the big particles (the ones with low-drug loading) significantly decreases size segregation tendencies. Using harsher milling conditions will cause all particles to be further normalized in size, which in turn will additionally reduce-size segregation. This, however, needs to be balanced with the need to maintain good powder flow properties, which in general tend to worsen as the particles size gets smaller.

Shear cell measurements

Mohr stress circle analysis (not shown) was employed to calculate the values of major principal stress ($\sigma 1$) and unconfined yield strength (σc) from which the critical flow factor ($ffc = \sigma 1/\sigma c$) was then calculated. The value of σc depends on the compacting stress in the bulk solid $\sigma 1$, and the relationship $\sigma c = f(\sigma 1)$ is called a flow function, a characteristic that is dependent on the powder properties. The value of cohesion (τc) was approximated as an intercept of linearized

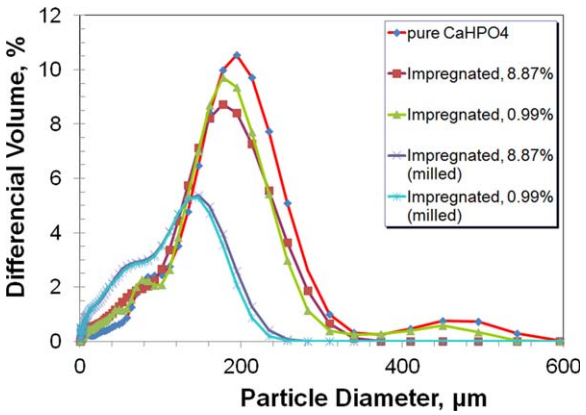

Figure 12. PSD measurements of pure, impregnated and impregnated and milled $CaHPO_4$.

[Color figure can be viewed in the online issue, which is available at wileyonlinelibrary.com.]

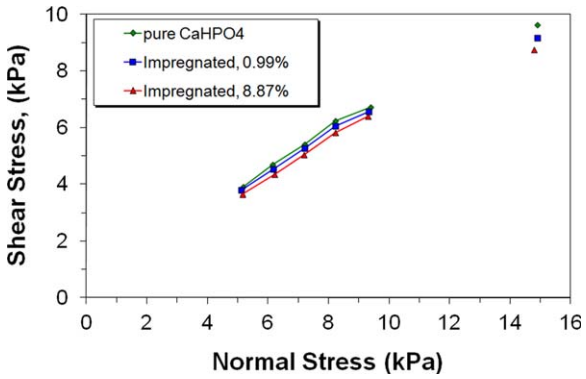

Figure 13. Shear-cell measurements by FT4 of pure and impregnated $CaHPO_4$.

[Color figure can be viewed in the online issue, which is available at wileyonlinelibrary.com.]

yield locus with the τ-axis. Changes in flow properties can be assessed by comparing the results for cohesion and critical flow factor. In general, the smaller the cohesion the better powders flow.[33] Similarly, the bigger the critical flow factor the better the flow.

Flow properties of pharmaceutical blends are an important factor affecting their formulation into final products (capsules or tablets). One of the main advantages of excipient impregnation with APIs is the ability to preserve the original flow properties of the pure excipient. In this section we examine this issue by analyzing and comparing shear cell data collected on pure and impregnated $CaHPO_4$. Figure 13 (yield locus) shows shear cell testing results of shear stress (τ) vs. normal stress (σ) for pure and impregnated $CaHPO_4$ (8.87% and 0.99%) as described in section "Analytical methods". All results from the Mohr stress circle analysis are presented in Table 6. Measured cohesion values are relatively low and decrease from $\tau_c = 0.432$ for pure $CaHPO_4$ to $\tau_c = 0.349$ for 0.99% impregnated $CaHPO_4$ and finally to $\tau_c = 0.173$ for 8.87% impregnated $CaHPO_4$. These data shows that all powders are free flowing, as suggested by the low-cohesion values. Cohesion decreases with increasing amount of API impregnated within the excipient, as suggested by the direction of change for the value of τ_c. The same trend can be concluded from the calculated *ffc* values. Although more testing is needed to firmly establish the aforementioned conclusions, the claim that impregnation preserves the original flow properties of the pure excipient can be confirmed with a high degree of certainty.

Often, flow properties are correlated to the Hausner ratio, a dimensionless number defined as the ratio of tapped density to bulk density of a powder. The Hausner ratio is viewed as an indirect measure of bulk density, size and shape, surface area, moisture and cohesiveness of

Table 6. Mohr Stress Circle Analysis Results for Shear Cell Measurements from Figure 13. Showing: UYS (σ_c) – Unconfined Yield Strength, MPS (σ_1) – Major Principle Stress, C (τ_c) – Cohesion, *ffc* (σ_1/σ_c) – Critical Flow Factor

Material	UYS, kPa	MPS, kPa	C	ffc
Pure $CaHPO_4$	1.64	26.5	0.432	16.2
Impregnated, 0.99%	1.32	25.2	0.349	19.1
Impregnated, 8.87%	0.652	24.2	0.173	37.1

Table 7. Bulk Densities, Tapped Densities and Hausner Ratios for Pure and Impregnated $CaHPO_4$ (Milled and Unmilled)

Material	Bulk Density, g/ml	Tapped Density, g/ml	Hausner Ratio
pure $CaHPO_4$	0.735	0.871	1.19
Impregnated, 8.87%	1.010	1.228	1.22
Impregnated, 0.99%	0.951	1.179	1.24
Milled&Impregnated, 8.87%	0.982	1.262	1.29
Milled&Impregnated, 0.99%	0.930	1.276	1.37

materials—all important physical properties of a powder that affect its flowability. Table 7 shows results for bulk and tapped densities for all materials presented in this article—pure $CaHPO_4$, impregnated $CaHPO_4$ and impregnated and milled $CaHPO_4$.

The data suggests a slight change in Hausner ratios from pure to impregnated excipient. This could be attributed to generation of fines during fluidization and impregnation because of attrition. Change in Hausner ratio to higher values for milled & impregnated $CaHPO_4$ is expected, as the particle size is intentionally reduced. The higher value for $CaHPO_4$ milled & impregnated to 0.99% (last in Table 7) could be attributed to the slightly smaller particles size as suggested by Figure 12. This is most likely due to slight differences in feed rate during milling.

From all the data in Table 7 it can be also concluded (as stated previously) that impregnation preserves the flow properties of pure excipient. It could be further stated that milling could be performed in a way that will slightly change bulk properties, yet still yield a free-flowing material with very high-blend uniformity, ideal for further formulation.

Tableting and compressibility study

All impregnated materials presented in this article were formulated in the form of filled hard gelatin capsules, which were in turn used to assess blend uniformity (section "Drug loading and blend uniformity") and dissolution profile (see section "Dissolution profile"). This formulation was chosen for its ease of manufacture and availability of appropriate equipment. It was interesting, however, to investigate the behavior of these materials if they were to be tableted, and to evaluate the resulting tablets. To achieve this with limited amounts of available materials, tablets were made using the Presster^{TM}, which is a tablet press replicator and compaction simulator. Materials used for tablet preparation included: pure $CaHPO_4$, impregnated $CaHPO_4$ (8.87% and 0.99%) and physical blends of $CaHPO_4$ and APAP with loadings 7.25% and 14.00%. All tablets produced for the comparison study were made with identical weight of 0.92 g without the introduction of any additive. Several tablets from each material were made by varying the compression force. Tablets were then measured for their thickness and hardness. Severe fracturing was observed for tablets made of pure $CaHPO_4$ and impregnated $CaHPO_4$ to 0.99%. In some case only the thickness was measured since the tablet was structurally compromised and hardness measurement would not have been accurate. Therefore, an incomplete set of data is presented for these two materials.

Figure 14 (upper plot) shows the results of tablet thickness vs. compression force. First we notice that pure $CaHPO_4$ and 0.99% impregnated behave almost identically, which is to be expected. There is not enough APAP loaded inside the excipient to cause any significant change. Second, we notice that tablet thickness for impregnated 8.87% CaHPO4 is lower than the one for the physical blend of lower loading (blend 7.25%). This is also to be expected as the API does not occupy the space between excipient particles (as it is the case with physical blends) but rather the space inside them (due to impregnation) resulting in smaller overall volume.

Figure 14 (lower plot) shows the results of tablet hardness vs. compression force. Pure $CaHPO_4$ is not shown as all tablets produced have shown severe fracturing and capping, making hardness measurements meaningless. The case was almost identical with material impregnated to low loading (0.99%) $CaHPO_4$, hence, only a few tablets were produced successfully. Regardless of the APAP content the two physical blends exhibited almost identical tablet hardness. However, impregnated $CaHPO_4$ to 8.89% shows much higher tablet hardness for the same compression force than the two blends. This suggests that APAP, when impregnated inside excipient particles, acts as a strong binder. The impregnation process strengthens the excipient particles within, making the tablet stronger.

Dissolution profile

The main propose of any pharmaceutical product is to appropriately deliver an API into the body. This is achieved by dissolving the API in the GI track from where it gets absorbed into the blood stream. Therefore, the dissolution

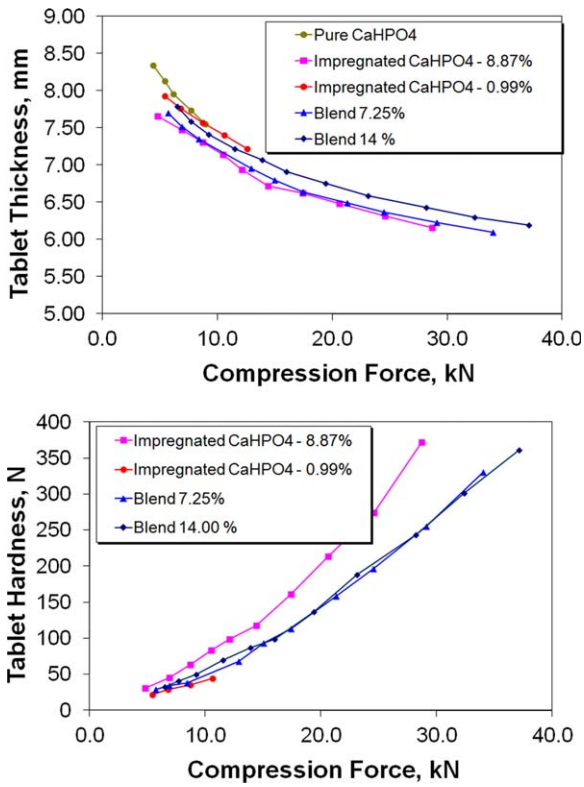

Figure 14. Tablet thickness vs. compression force (top), and tablet hardness vs. compression force (bottom) for tablets made of pure $CaHPO_4$, impregnated $CaHPO_4$ (0.99% and 8.87% loadings) and various blends of $CaHPO_4$ with APAP.

[Color figure can be viewed in the online issue, which is available at wileyonlinelibrary.com.]

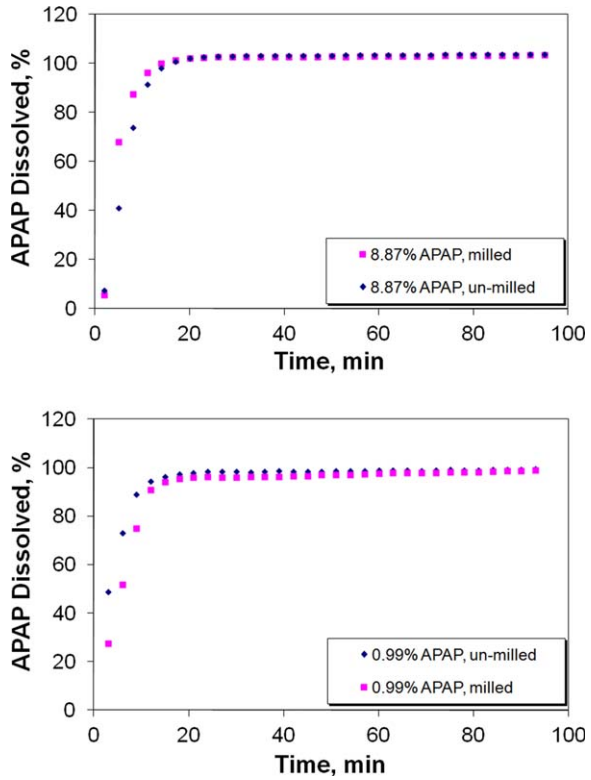

Figure 15. Dissolution profiles of gelatin capsules filled with impregnated $CaHPO_4$ (unmilled and milled) with APAP to 8.87% loading (top) and 0.99% loading (bottom) in aqueous media with pH 5.8 (phosphate buffer).

[Color figure can be viewed in the online issue, which is available at wileyonlinelibrary.com.]

profile becomes an important characteristic of any pharmaceutical formulation and measuring it, an integral part of any drug product development. The *in vitro* release profile of APAP from impregnated blends with 8.87% and 0.99% loading was studied. All measurements were performed in accordance with the USP method for APAP filled capsules: apparatus I, basket method, phosphate buffer with pH = 5.8. According to the USP method for acetaminophen (capsules or tablets), the release of the API should take 30 min or less. Impregnated $CaHPO_4$ to 0.1% loading was not tested due to detection limitations of the instrument. It should be mentioned that at these conditions the excipient remained undissolved throughout the test. All gelatin capsules disintegrated after about a minute and this time was factored in the final results.

Figure 15 (top) shows release profile for milled and unmilled impregnated $CaHPO_4$ to 8.87% APAP. Both dissolution profiles meet the USP requirement of 80% release in 30 min or less. The data shows slightly faster release for milled material. Release of 80% of APAP in the milled case is around 7 min vs. 9 min for the un-milled case. Figure 15 (bottom) shows release profile for milled and unmilled impregnated $CaHPO_4$ to 0.99% APAP. Again the USP requirement for APAP release is quickly met for both materials. For these two cases data suggests slightly faster dissolution for un-milled $CaHPO_4$. The required 80% release of APAP is achieved in about 7 min for unmilled vs. 10 min for milled $CaHPO_4$.

Conclusions

The aim of this work was to present a study on a new method for formulation and manufacture of pharmaceuticals by fluidized-bed impregnation of APIs onto porous excipients. This article discusses a limited number of results for a fairly small set of parameters. Further work is needed to explore the full range of parameters and to investigate optimization of variables. The proposed method has operational simplicity and offers several advantages over conventional techniques. The study in this article involved acetaminophen as the model drug and anhydrous dibasic calcium phosphate as the porous excipient, but the methods presented here can be used for many other drugs and carriers with minimum modification.

Fluidized-bed impregnation can be summarized as the combination of three distinct processes taking place simultaneously. These include fluidization of the porous carrier, spraying API solution within the bed, which penetrates the excipient due to capillary forces, and drying of the porous particles causing the API to be deposited within. Final API loading is not limited by its solubility in the organic solvent. Lower solubility could be compensated with longer run times to achieve targeted loadings.

This study helped to establish the following claims about impregnating APAP into anhydrous $CaHPO_4$ using fluidized bed:

- Successful proof of concept.
- Ability of the process to deliver final product with high blend uniformity (as expressed in %RSD), independent of the API loading.
- Milling of the impregnated material further improves blend uniformity.
- Physical state of impregnated APAP inside porous excipient is crystalline.
- FB impregnation process by design preserves the final bulk physical properties and flow properties of the impregnated materials compared to those of the pure excipient.
- Impregnated APAP acts as a binder during tableting, making harder tablets when compared to physical blends.
- FB impregnation does not slow down the dissolution profile of APAP.
- FB impregnation is a fast, one-step process that is able to deliver final pharmaceutical material ready for formulation into capsules (or tablets).

Implementing fluidized-bed impregnation in drug manufacturing could allow for significant cost savings due to elimination of several unit operations. These include steps to control API attributes (secondary crystallization, milling), steps to control flow properties of final blends (mixing with various additives) or steps to control blend uniformity (wet or dry granulation, roller compaction). Fluidized-bed impregnation by design does not depend on the nature of the API but rather on the nature of the excipient used. Proper design of the porous excipient could potentially allow its universal use with a variety of APIs.

Acknowledgments

We would like to thank Xue Liu and Golshid Keyvan for assistance.

Literature Cited

1. Nickerson B. *Sample Preparation of Pharmaceutical Dosage Forms: Challenges and Strategies for Sample Preparation and Extraction.* American Association Pharmaceutical Scientists; 2011:145.

2. Zheng J. *Formulation and Analytical Development for Low-Dose Oral Drug Products*. Hoboken, NJ: John Wiley & Sons, Inc.; 2009.
3. FDA. Guidance for Industry: Powder blends and finished dosage units – stratified in-process dosage unit sampling and assessment. http://www.fda.gov/downloads/Drugs/GuidanceComplianceRegulatoryInformation/Guidances/ucm070312.pdf. October 2003.
4. Lee SY, Aris R. The distribution of active ingredients in supported catalysts prepared by impregnation. *Catal Rev Sci Eng*. 1985;27(2): 207–340.
5. Komiyama M. Design and preparation of impregnated catalysts. *Catal Rev Sci Eng,* 1985;27(2):341–372.
6. Neimark AV, Kheifets LI, Fenelonov VB. Theory of preparation of supported catalysts. *Ind Eng Chem Product Res Develop*. 1981; 20(3):439–450.
7. Gavriilidis A, Varma A, Morbidelli M. Optimal distribution of catalyst in pellets. *Catal Rev Sci Eng*. 1993;35(3):399–456.
8. Maatman RW, Prater CD. Adsorption and exclusion in impregnation of porous catalytic supports. *Ind Eng Chem*. 1957;49(2):253–257.
9. Lekhal A, Glasser BJ, Khinast JG. Impact of drying on the catalyst profile in supported impregnation catalysts. *Chem Eng Sci*. 2001; 56(15):4473–4487.
10. Liu, X, Khinast JG, Glasser BJ. Drying of supported catalysts: A comparison of model predictions and experimental measurements of metal profiles. *Ind Eng Chem Res*. 2010;49(6):2649–2657.
11. Liu X, Khinast V, Glasser BJ. A parametric investigation of impregnation and drying of supported catalysts. *Chem Eng Sci*. 2008; 63(18):4517–4530.
12. Mellaerts R, Jammaer JAG, Van Speybroeck M, Chen H, Van Humbeeck J, Augustijns P, Van den Mooter G, Martens JA. Physical state of poorly water soluble therapeutic molecules loaded into SBA-15 ordered mesoporous silica carriers: A case study with itraconazole and ibuprofen. *Langmuir*. 2008;24(16):8651–8659.
13. Van Speybroeck M, Barillaro V, Do Thi T, Mellaerts R, Martens J, Van Humbeeck J, Vermant J, Annaert P, Van Den Mooter G, Augustijns P. Ordered mesoporous silica material SBA-15: A broad-spectrum formulation platform for poorly soluble drugs. *J Pharma Sci*. 2009;98(8):2648–2658.
14. Rengarajan GT, Enke D, Steinhart M, Beiner M. Stabilization of the amorphous state of pharmaceuticals in nanopores. *J Mater Chem*. 2008;18(22):2537–2539.
15. Ji CD, Barrett A, Poole-Warren LA, Foster NR, Dehghani F. The development of a dense gas solvent exchange process for the impregnation of pharmaceuticals into porous chitosan. *Int J Pharma*. 2010;391(1-2):187–196.
16. Lopez-Periago A, Argemi A, Andanson JM, Fernandez V, Garcia-Gonzalez CA, Kazarian SG, Saurina J, Domingo C. Impregnation of a biocompatible polymer aided by supercritical CO(2): Evaluation of drug stability and drug-matrix interactions. *J Supercrit Fluids*. 2009; 48(1):56–63.
17. Verraedt E, Pendela M, Adams E, Hoogmartens J, Martens JA. Controlled release of chlorhexidine from amorphous microporous silica. *J Controlled Release*. 201;142(1):47–52.
18. Chevalier E, et al. Ibuprofen-loaded calcium phosphate granules: Combination of innovative characterization methods to relate mechanical strength to drug location. *Acta Biomaterialia*. 2010;6(1): 266–274.
19. Ugaonkar S, Needham TE, Bothun GD. Solubility and partitioning of carbamazepine in a two-phase supercritical carbon dioxide/polyvinylpyrrolidone system. *Int J Pharma*. 2011;403(1-2):96–100.
20. Banchero M, Manna L, Ronchetti S, Campanelli P, Ferri A. Supercritical solvent impregnation of piroxicam on PVP at various polymer molecular weights. *J Supercrit Fluids*. 2009;49(2):271–278.
21. Beiner M, Rengarajan GT, Pankaj S, Enke D, Steinhart M. Manipulating the crystalline state of pharmaceuticals by nanoconfinement. *Nano Lett*. 2007;7(5):1381–1385.
22. Desportes S, Steinmetz D, Hemati M, Philippot K, Chaudret B. Production of supported asymmetric catalysts in a fluidised bed. *Powder Technol*. 2005;157(1-3):12–19.
23. Barthe L, Desportes S, Hemati M, Philippot K, Chaudret B. Synthesis of supported catalysts by dry impregnation in fluidized bed. *Chem Eng Res Des*. 2007;85(A6):767–777.
24. Barthe L, Hemati M, Philippot K, Chaudret B. Dry impregnation in fluidized bed: Drying and calcination effect on nanoparticles dispersion and location in a porous support. *Chem Eng Res Des*. 2008; 86(4A):349–358.
25. Barthe L, Desportes S, Steinmetz D, Hemati M. Metallic salt deposition on porous particles by dry impregnation in fluidized bed: Effect of drying conditions on metallic nanoparticles distribution. *Chem Eng Res Des*. 2009;87(7A): 915–922.
26. Muzzio FJ, Shinbrot T, Glasser BJ. Powder technology in the pharmaceutical industry: the need to catch up fast. *Powder Technol*. 2002;124(1-2):1–7.
27. Muzzio FJ, Glasser BJ, Grigorov PI. Formulation and manufacture of pharmaceuticals by impregnation onto porous carriers (WO 2012027222 A1); 2011.
28. Miyazaki T, Sivaprakasam K, Tantry J, Suryanarayanan R. Physical characterization of dibasic calcium phosphate dihydrate and anhydrate. *J Pharma Sci*. 2009;98(3): 905–916.
29. Carson JW, Wilms H. Development of an international standard for shear testing. *Powder Technol*. 2006;167(1):1–9.
30. Freeman R. Measuring the flow properties of consolidated, conditioned and aerated powders - A comparative study using a powder rheometer and a rotational shear cell. *Powder Technol*. 2007;174(1-2):25–33.
31. Doldan C, Souto C, Concheiro A, Martinezpacheco R, Gomezamoza JL. Dicalcium phosphate dihydrate and anhydrous dicalcium phosphate for direct compression - a comparative-study. *Int J Pharma*. 1995;124(1):69–74.
32. Alcoutlabi M, McKenna GB. Effects of confinement on material behaviour at the nanometre size scale. *J Phys Condensed Matter*. 2005;17(15):R461–R524.
33. Vasilenko A, Glasser BJ, Muzzio FJ. Shear and flow behavior of pharmaceutical blends - Method comparison study. *Powder Technol*. 2011;208(3):628–636.

Manuscript received July 11, 2012, revision received Apr. 30, 2013, and final revision received July 20, 2013.